

SUPPORTING INFORMATION

Proximity Proteomics Has Potential for Extracellular Vesicle Identification

Hisako Kaneda^{1,2}, Yui Ida¹, Ryusuke Kuwahara³, Izumi Sato¹, Takanari Nakano¹, Haruhiko Tokuda⁴, Tsuyoshi Sato², Takayuki Murakoshi¹, Koichi Honke⁵, and Norihiro Kotani^{1*}

- 1 Department of Biochemistry, Saitama Medical University, 38 Morohongo, Moroyama-machi, Iruma-gun, Saitama, 350-0495, Japan
- 2 Department of Oral and Maxillofacial Surgery, Saitama Medical University, 38 Morohongo, Moroyama-machi, Iruma-gun, Saitama, 350-0495, Japan
- 3 Quantum Wave Microscopy Unit, Okinawa Institute of Science and Technology Graduate University, 1919-1 Tancha, Onna-son, Kunigami-gun, Okinawa, 904-0495, Japan
- 4 Medical Genome Center Biobank, National Center for Geriatrics and Gerontology, 7-430 Morioka-cho, Obu, Aichi, 474-8511, Japan
- 5 Department of Biochemistry, Kochi University Medical School, Nankoku, Kochi, 783-8505, Japan

*corresponding author email address: kotani@saitama-med.ac.jp

Figure S1. EMARS reaction

Figure S2. Expression of CHL1 and other partner proteins in precipitated serum EVs

Figure S3. Confirmation of proteins with mouse serum CHL1-EVs

Figure S4. Characterization of ELISA system for SLC4A1

Figure S5. ROC and scatter-plot analysis of SLC4A1 ELISA

Figure S6. Measurement of CHL1-SLC4A1 EV in human serum EVs

Figure S7. Characterization of ELISA for fluorescein labeled-caspase 14

Figure S8. Western blotting images of the entire membrane in this study

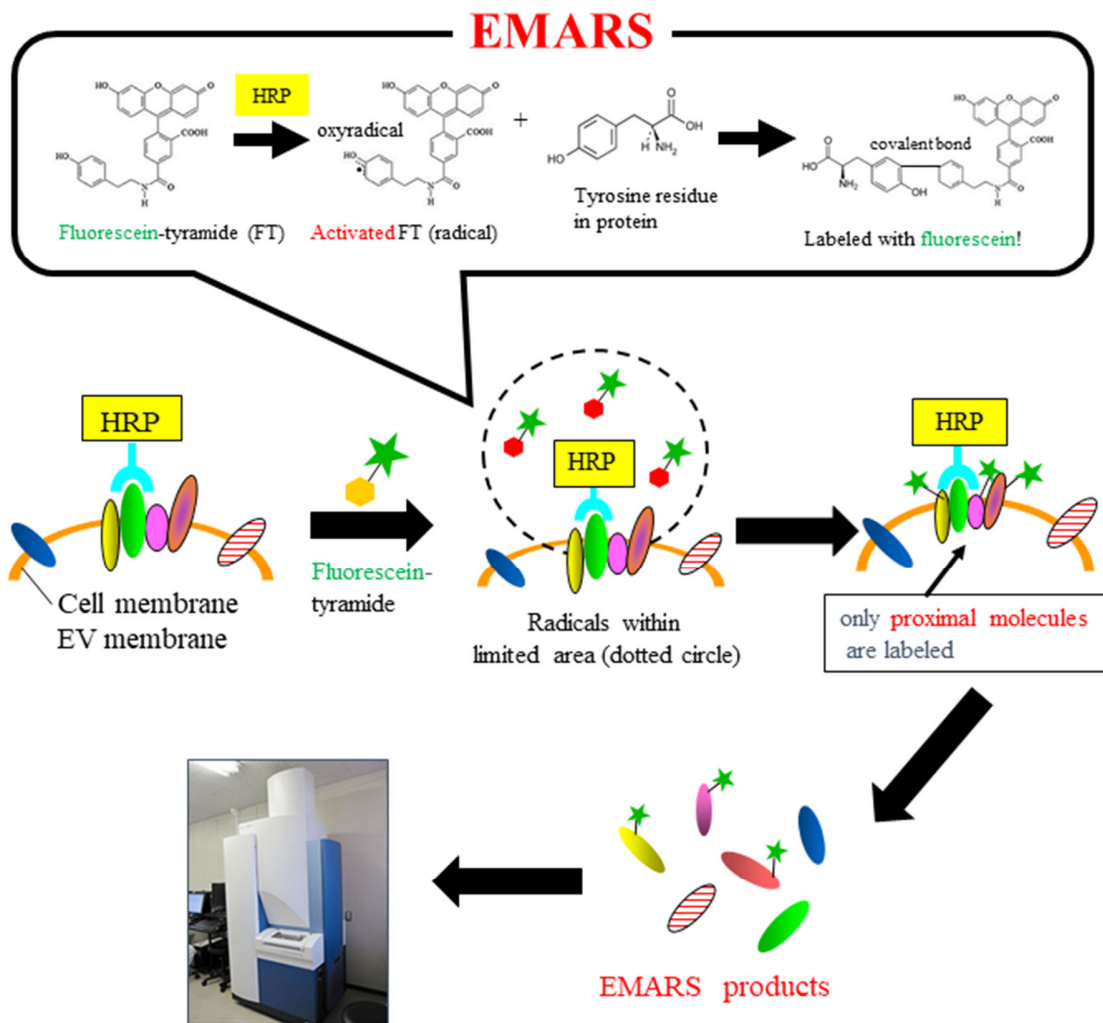
Table S1 Mass spectrometry system parameters and search parameters used in this study

Table S2 Detailed data of WT and EML4-ALK TG mice used in proteome analysis

Table S3 Candidate proteins in serum CHL1-EVs from WT, TL, and TS mice

Table S4 Clinical data of healthy person and lung cancer patients providing serum

Table S5 Candidate proteins in CHL1-EVs from H and LC patients



**Identification of ★-tagged proteins
by proteomic analysis**

Figure S1. EMARS reaction

Schematic illustration of the EMARS reaction using fluorescein-tyramide (FT). HRP-conjugated cognitive molecules (e.g., antibodies) recognizing the given molecule were prepared (“EMARS probe”) and added to living cells, followed by treatment with FT. After the EMARS reaction, the sample proteins (“EMARS products”) were subjected to gel electrophoresis and/or mass spectrometry analysis for the purification of fluorescein-labeled proteins as proximity molecules.

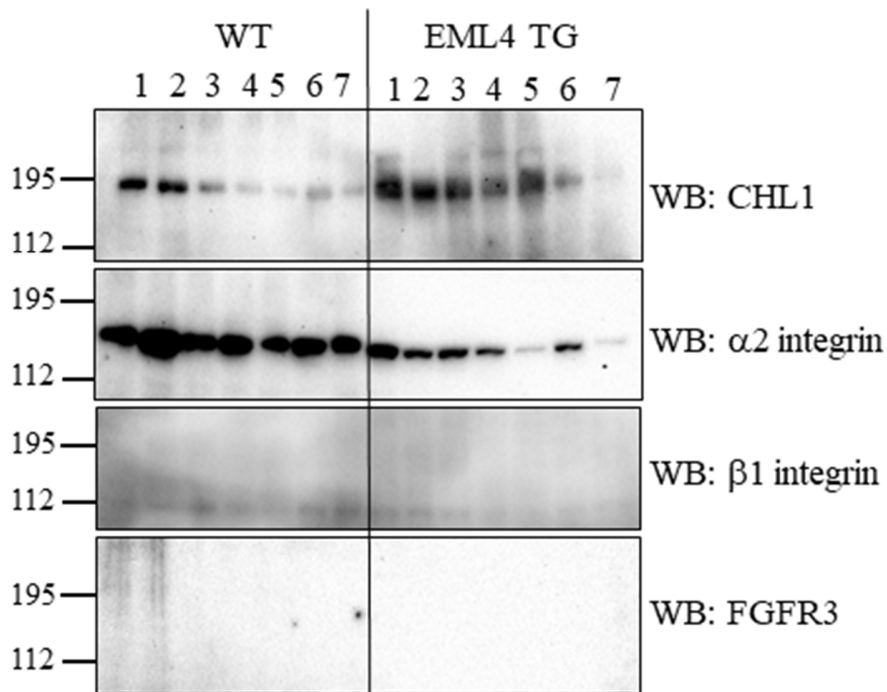


Figure S2. Expression of CHL1 and other partner proteins in precipitated serum EVs

Protein expression of precipitated serum EVs from wild-type (WT) and *EML4-ALK* transgenic mice (TL group). The serum EVs collected from seven WT and TL mice were subjected to western blot analysis with anti-CHL1, anti- α 2 integrin, anti- β 1 integrin, and anti-FGFR3 antibodies, previously reported as cancer cell membrane BiCAT molecules.

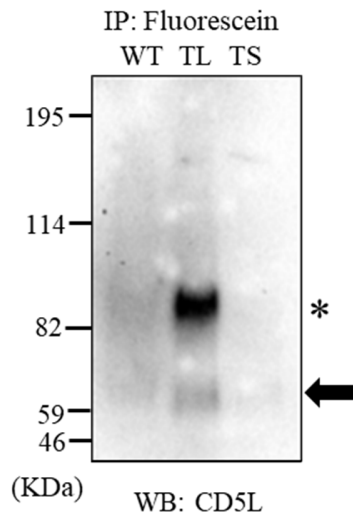


Figure S3. Confirmation of proteins with mouse serum CHL1-EVs

Immunoprecipitation and western blot analysis of candidate partner molecules (CD5L) with mouse CHL1 in EVs. The EMARS products of WT, TL, and TS were subjected to immunoprecipitation (anti-fluorescence antibody Sepharose) and western blot analysis with anti-CD5L antibody. Arrows indicate the bands of CD5L proteins. The asterisk indicates unknown bands (predicted as non-specific or partial fragments).

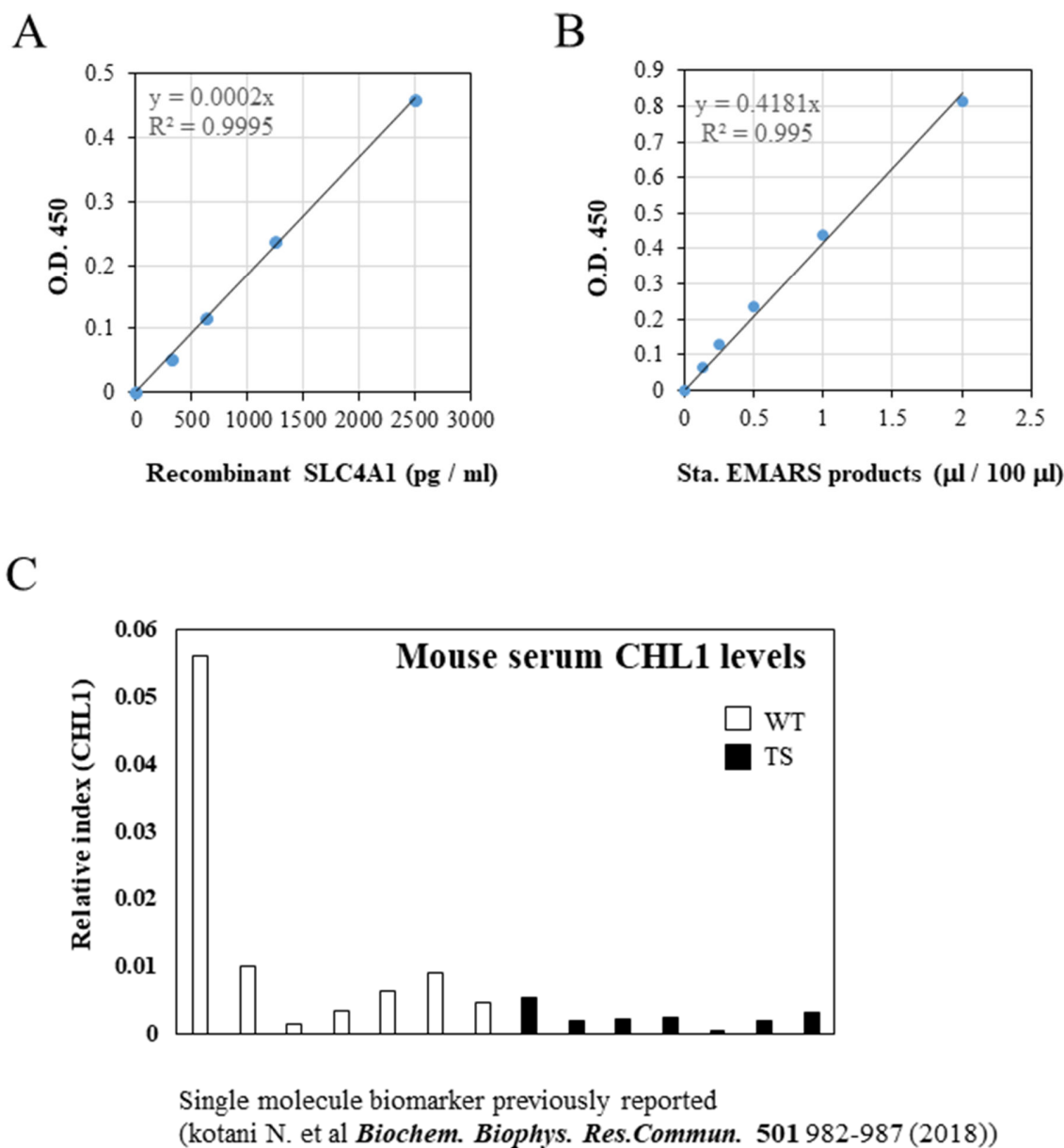


Figure S4. Characterization of ELISA system for SLC4A1

(A, B) Calibration curve of sandwich ELISA for the detection of both SLC4A1 partial proteins and fluorescein-labeled SLC4A1. The detection of several concentrations of recombinant SLC4A1 partial protein using HRP-labeled anti-SLC4A1 antibody, which was prepared using the Zenon system, is summarized in (A). The detection of several concentrations of self-made standard materials containing fluorescein-labeled SLC4A1 using HRP-labeled anti-fluorescein antibody is summarized in (B). (C) Comparison of serum CHL1 levels between wild-type (WT) and small tumor-bearing *EML4-ALK* transgenic (TS) mice using a previously established ELISA system for CHL1 measurement. No significant differences were observed between the groups.

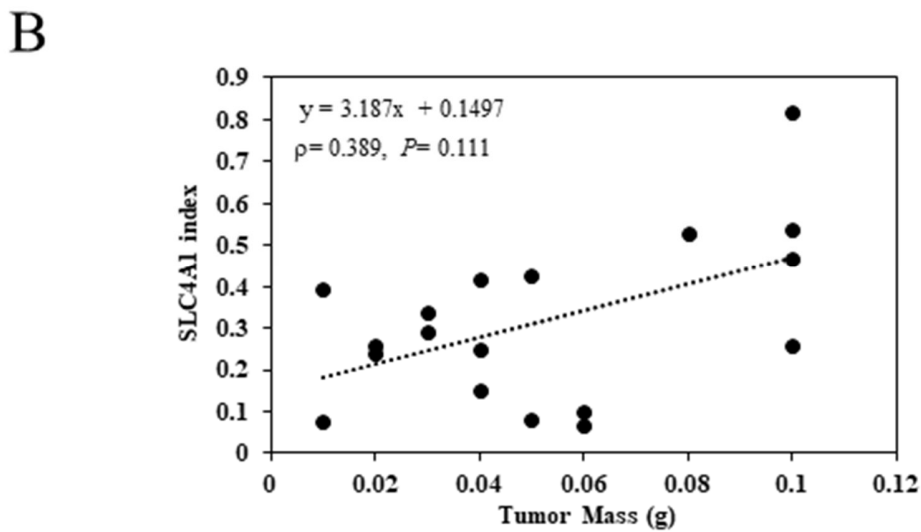
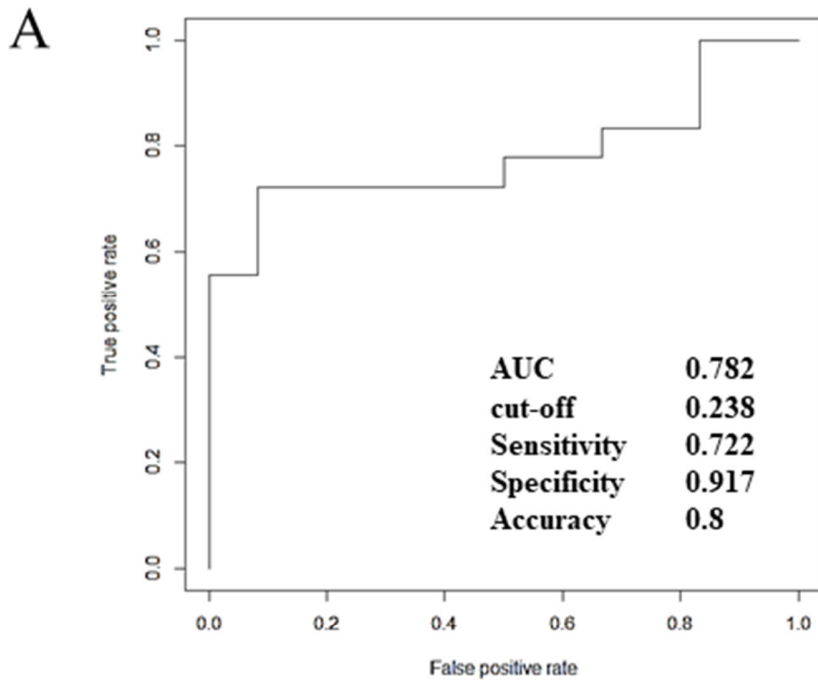
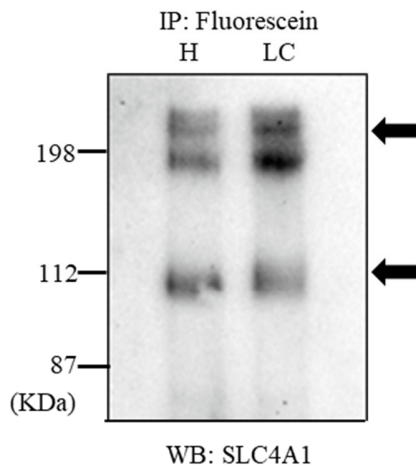


Figure S5. ROC and scatter-plot analysis of SLC4A1 ELISA

(A) ROC curve for the SLC4A1 indexes. The AUC was calculated as 0.782. (B) Scatterplot of tumor mass versus SLC4A1 index. The correlation between the SLC4A1 index and lung tumor mass of TS was estimated using Spearman's rank correlation coefficient (0.389, $p = 0.111$).

A



B

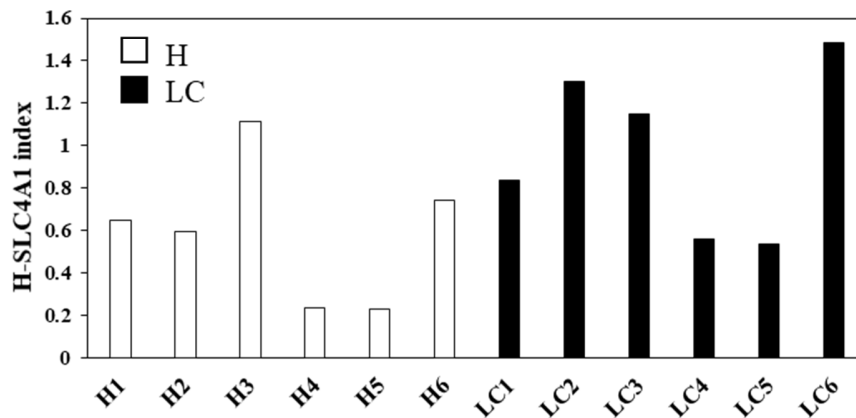
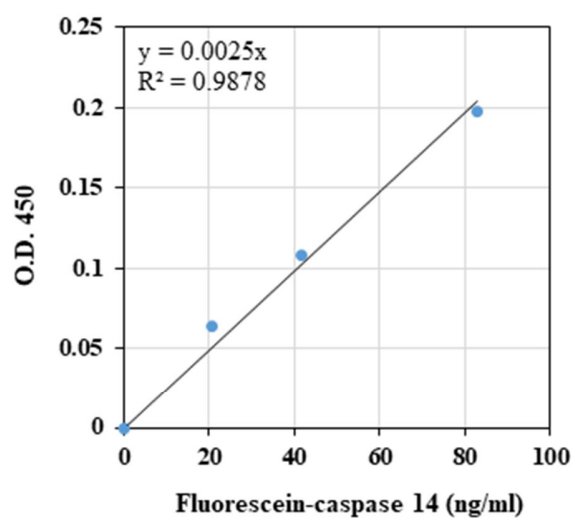


Figure S6. Measurement of CHL1-SLC4A1 EV in human serum EVs

(A) EMARS samples from healthy individuals (H) and lung cancer patients (LC) were subjected to immunoprecipitation (anti-fluorescence antibody Sepharose) and western blot analysis with anti-SLC4A1 antibody, respectively. Arrows indicate the detected bands of human SLC4A1 proteins (including predicted dimers). (B) Measurement of fluorescein-labeled human SLC4A1 using a sandwich ELISA system in mouse fluorescein-labeled SLC4A1. The serum EVs from 6 H (open bar) and 6 LC (closed bar) were applied to the EMARS reaction, followed by ELISA measurement. The EMARS products containing fluorescein-labeled SLC4A1 were added to anti-SLC4A1 antibody-coated ELISA plates. “H-SLC4A1 index” was calculated based on the value of fluorescein-labeled SLC4A1 in standard samples as described in the Experimental procedures.

A



B

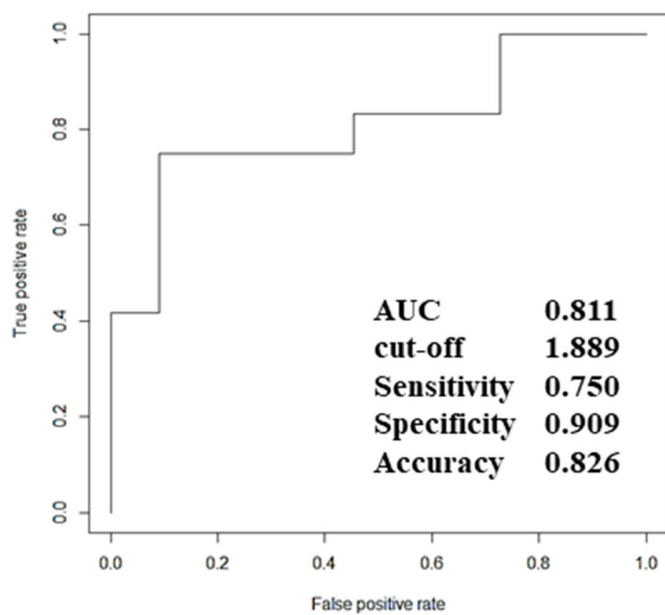


Figure S7. Characterization of ELISA for fluorescein labeled-caspase 14

(A) The calibration curve of sandwich ELISA for the detection of fluorescein-labeled caspase 14. The detection of several concentrations of fluorescein-labeled caspase 14 standard was performed using an HRP-labeled anti-fluorescein antibody. (B) ROC curve for the caspase 14 indexes. The AUC was calculated to be 0.811.

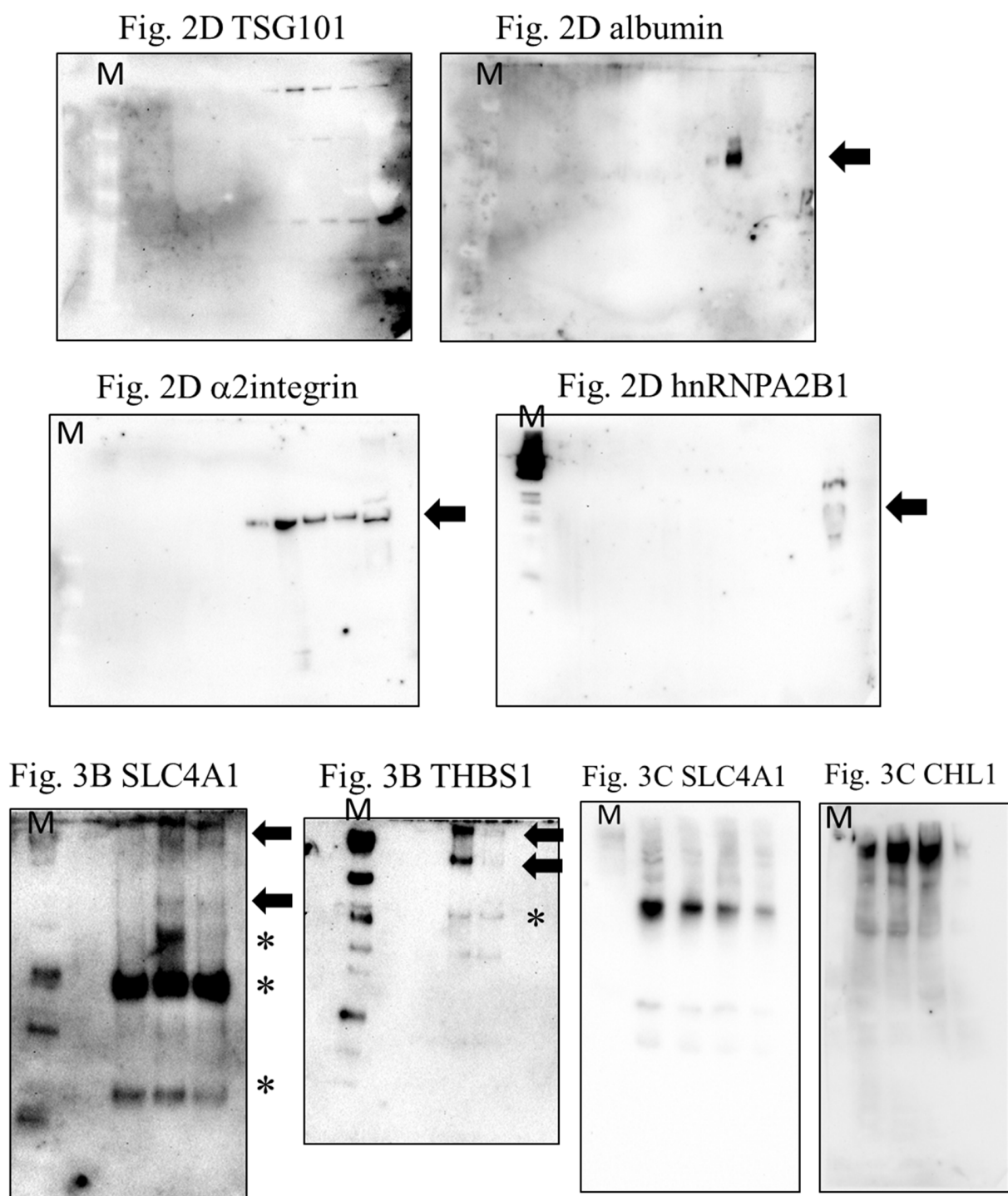


Figure S8. Western blot images of the entire membrane in this study

Lane “M” indicates molecular marker lane. Arrows indicate the bands of target protein(s). The asterisk indicates unknown bands (predicted as from non-specific protein, partial fragments of target molecule, and IgG fragments from IP antibodies).

Figure S8. continue-

Fig. 3D SLC4A1

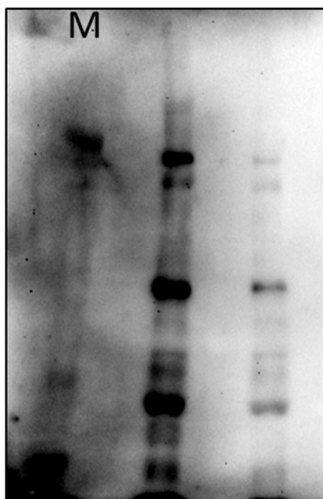


Fig. 4B caspase14

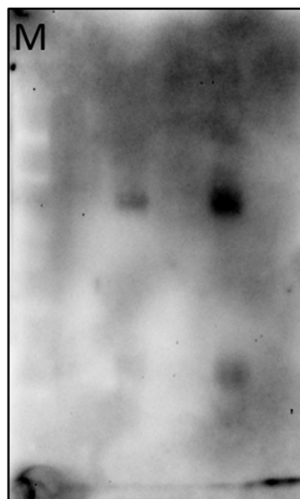


Fig. 4C caspase14

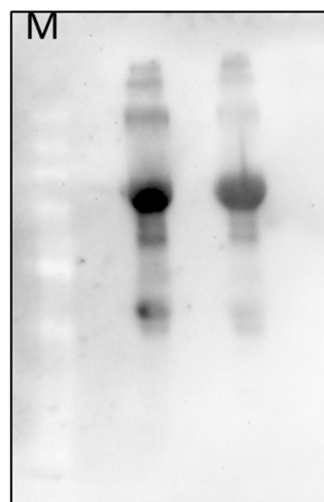


Fig. S2 mCHL1

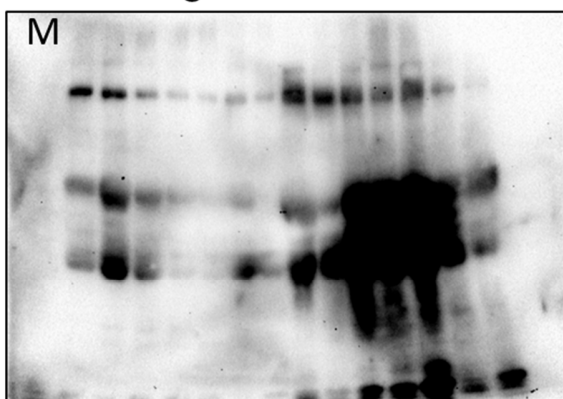


Fig. S2 α 2 integrin

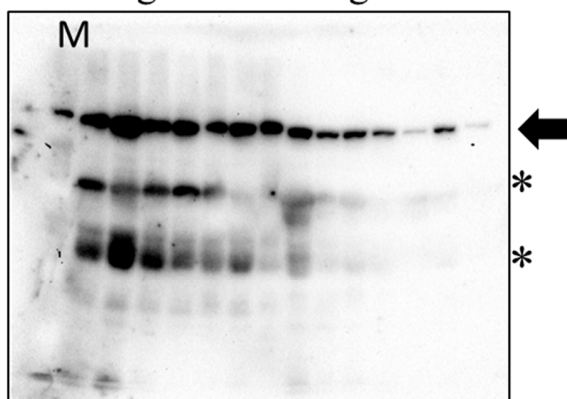


Fig. S2 β 1 integrin

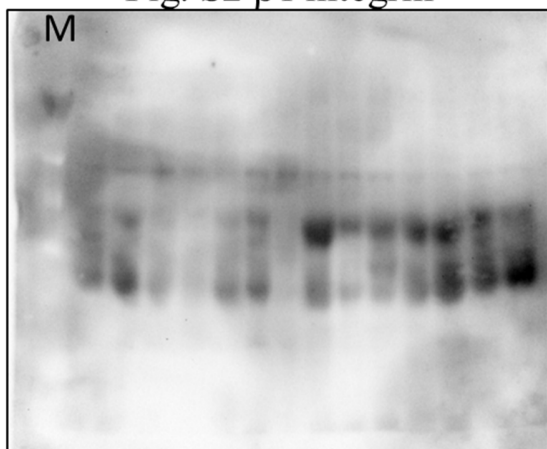


Fig. S2 FGFR3

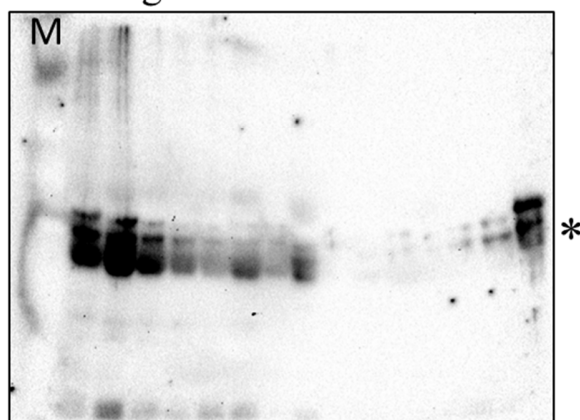


Figure S8. continue-

Fig. S3 CD5L

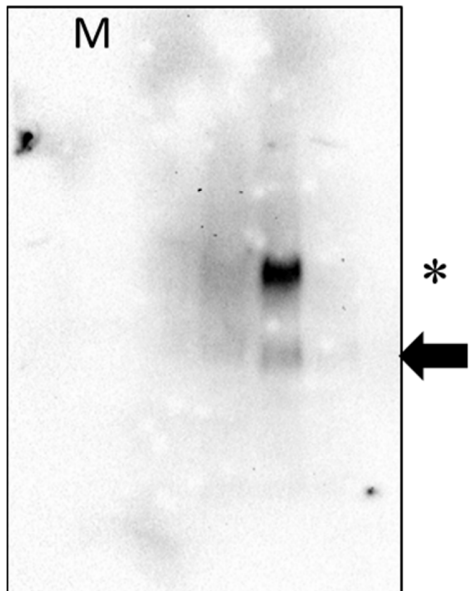


Fig. S6 SLC4A1

